GFP-mut2 Proteins in Trehalose-Water Matrixes: Spatially Heterogeneous Protein-Water-Sugar Structures

Laura D'Alfonso,*¶ Maddalena Collini,*¶ Fabio Cannone,*¶ Giuseppe Chirico,*¶ Barbara Campanini,†‡ Grazia Cottone,§¶ and Lorenzo Cordone§¶

*Dipartimento di Fisica, Università di Milano Bicocca, Milano, Italy; †Dipartimento di Biochimica e Biologia Molecolare, Università di Parma, Parma, Italy; ‡Dipartimento di Sanità Pubblica, Università di Parma, Parma, Italy; §Dipartimento di Scienze Fisiche e Astronomiche, Università di Palermo, Palermo, Italy; and ¶Consorzio Nazionale Interuniversitario Per Le Scienze Fisiche Della Materia, Roma, Italy

ABSTRACT   We report investigations on the properties of nanoenvironments around single-GFP-mut2 proteins in trehalose-water matrixes. Single-GFPmut2 molecules embedded in thin trehalose-water films were characterized in terms of their fluorescence brightness, bleaching dynamics, excited state lifetime, and fluorescence polarization. For each property, sets of ~100–150 single molecules have been investigated as a function of trehalose content and hydration. Three distinct and interconverting families of proteins have been found which differ widely in terms of bleaching dynamics, brightness, and fluorescence polarization, whose relative populations sizably depend on sample hydration. The reported results evidence the simultaneous presence of different protein-trehalose-water nanostructures whose rigidity increases by lowering the sample hydration. Such spatial inhomogeneity is in line with the well-known heterogeneous dynamics in supercooled fluids and in nonsolid carbohydrate glasses and gives a pictorial representation of the sharp, sudden reorganization of the above structures after uptake ⇆ release of water molecules.

INTRODUCTION

Trehalose is a nonreducing disaccharide of glucose found in large quantities in organisms which can survive in extreme drought and high temperature under a condition in which metabolic processes are fully absent known as anhydrobiosis. Such organisms can remain under anhydrobiosis for several years and, upon rehydration, their vegetative cycles restart. Organisms in anhydrobiosis exhibit large resistance to stress factors. Preservation against adverse conditions has also been observed for isolated systems such as proteins or liposomes embedded in trehalose-containing matrixes (1–7).

Experiments (8–17) and molecular dynamics (MD) simulations (18) have shown that when proteins are embedded in trehalose-containing matrixes of low water content, the large-scale internal motions, which in glycerol-water start above ~180 K, are strongly inhibited. Furthermore, Fourier transform infrared spectroscopy measurements (19–24) and MD simulations (25,26) on carboxy-myoglobin (MbCO) embedded in water-trehalose matrixes allowed us to infer the existence of water molecules, at the protein interface, which are involved in hydrogen-bond (HB) networks whose rigidity increases by decreasing the sample water content. Such networks anchor the protein to its surroundings, thus coupling the degrees of freedom of the protein to those of the external matrix. Furthermore, it was observed that protein continuous photoexcitation temporarily destroys the hard HB network in dry samples (light-induced relaxation) but does not affect the soft HB network in hydrated samples (16,17,27).

Hochstrasser and co-workers (28) studied, at the single-molecule level, the internal dynamics of Rhodamine 6G and cytochrome c embedded in thin trehalose films (prepared by spin coating proteins dissolved in solutions of a water/trehalose molar ratio $\cong 2$) and reported a heterogeneous dynamics of both the dye and the protein. Based on the notion that the hardness of the HB network, which couples the protein to the external matrix, is modulated by the sample water content, we thought it relevant to extend the single-molecule study to samples in which proteins are embedded in trehalose-water matrixes of different sugar content and hydration: this enabled us to obtain knowledge on the distribution of the protein dynamic behaviors as a function of the sample composition. Accordingly, we characterized single green fluorescent protein-mut2 (GFPmut2) molecules embedded in thin trehalose-water films in terms of their fluorescence brightness, bleaching dynamics, excited state lifetime, and fluorescence polarization anisotropy.

MATERIALS AND METHODS

Chemicals

All chemicals (except trehalose) were purchased from Sigma-Aldrich (St. Louis, MO) and were used without further purification. Trehalose from Hayashibara Shoij (Okayama, Japan) was used after recrystallization from aqueous solutions. Experiments were carried out at room temperature.

Protein

GFPmut2 is a mutant of green fluorescent protein (GFP) containing a triple substitution (S65A, V68L, S72A) which confers enhanced fluorescence emission and high yield of protein expression due to a more efficient folding

at 37°C (29). Fluorescence is ascribed to the intrinsic chromophore (30) and can be taken as a marker for the structural integrity of the protein (31–34).

GFPmut2 expression and purification

The GFPmut2 gene, cloned in a pKEN1 vector (35), was kindly provided by Dr. Brendan P. Cormack (Department of Microbiology and Immunology, Stanford University School of Medicine, Stanford, CA) (36). Protein expression and purification was carried out as previously described (37); GFPmut2 stock solutions were dialyzed against 50 mM Tris buffer, pH 8.0, and kept at −80°C.

Sample preparation

GFP mut2 molecules, dissolved in a phosphate buffer saline pH 6.8 buffer, were diluted at ~100 nM concentration in trehalose solutions of increasing sugar/water ratio (0%, 5%, 10%, and 35% w/w). Aliquots of ~2 μl of the mixture were deposited on a glass slide and spin coated under vacuum. Samples were then dried at 60°C right before the measurements. We took particular care in preparing spin-coated samples starting from solutions of identical composition, except for the trehalose concentration, when needed.

Optical setup

The two-photon excitation (TPE) setup was based on a mode-locked Ti:sapphire laser (Tsunami 3960, Spectra Physics, Mountain View, CA) coupled to a Nikon (Tokyo, Japan) TE300 microscope. The lasers provide 280-fs pulses on the sample plane (38) at a repetition frequency of 80 MHz in the range 720–950 nm. Optical collection is based on a piezo raster scanning unit adapted for TPE (39). The fluorescence signal, collected by a Plan Apochromat 100× oil objective (numerical aperture = 1.3, Nikon) and selected by an emission band-pass filter (HQ515-30, emission at 515 nm, full width of 30 nm, Chroma, Brattelboro, VT), is fed directly to two single-photon avalanche diode (SPAD) modules (Perkin-Elmer, Vaudreuil, Quebec, Canada; model SPCM-AQR15) by splitting the fluorescence signal by means of a nonpolarizing 50% or polarizing cube, as needed. The radial and axial profiles are 240 ± 40 nm and 780 ± 50 nm, respectively (39). The excitation intensity on the sample is computed as the average power divided by the area of the point spread function in the focal plane (1 mW corresponds to ~400 kW/cm^2).

Fluorescence properties of GFPmut2 protein

The TPE spectrum of GFPmut2 encapsulated in silica gels exhibits two main components at 820 ± 2 and 885 ± 3 nm and a shoulder at ~760 nm. The relative amplitude of the 820- and 885-nm bands changes with pH (40). The excitation at 885 nm is largely favored at high pH with respect to the band at 820 nm, suggesting that the 885-nm excitation band is due to the two-photon absorption of the anionic state of the GFPmut2 chromophore; whereas the excitation at 820 nm corresponds to the absorption of the neutral chromophore. The TPE emission, upon excitation at 820 nm, shows three bands at 456, 510, and 538 nm, in good agreement with the one-photon emission (OPE) spectra (41). The major component at 510 nm corresponds to the one-photon absorption at 485 nm (41) and is ascribed to the anionic state of the chromophore. The emission at ~460 nm is due to the neutral state of the chromophore (41).

Fluorescence spectroscopy on single molecules

Single GFP molecules were selected by performing fast fluorescence images (excitation wavelength = 860 nm, emission filter = 515 ± 15 nm) and by analyzing the histogram of the emission signal as described in detail

elsewhere (42). Images (100 × 100 pixels) were acquired with a pixel dwell time of 1 ms per pixel, field of view ≅ 5 × 5 μm and variable excitation power on the sample from ≅10 up to 100 kW/cm^2. A quarter wavelength plate was inserted in the excitation optical path at 45° to the excitation polarization to obtain isotropic excitation of the protein absorption dipole. With such parameters, one single-molecule spot corresponds to ~4 × 4 pixels. Axial scanning ensured that the field under observation was unaltered during the long-lasting experiments. Fields containing only 5–30 GFPmut2 molecules (37,43) were usually considered for the analysis. For good statistics, ~100–150 single molecules were examined. Unless otherwise specified, on each spot we collected the full fluorescence emission with 1-ms time resolution up to the bleaching time, T_B, which is the time at which a sudden, complete, and permanent loss of fluorescence emission occurs (44). Of course, we cannot rule out an emission recovery after a time longer than the observation time of our experiment. Moreover, we stress that the reported T_B values are the "absolute bleaching times", i.e., the overall spells of time, which include the time intervals in which the molecule does not fluoresce due to blinking (45). Then, only data collected from spots whose traces show a single stepwise, "permanent", drop of the signal were considered in the subsequent analysis, since this behavior is considered one of the fingerprints of single-molecule emission (42). The excitation power of 25 microwatts (intensity ≅10 kW/cm^2) has been routinely used since it allowed us to keep the uncertainty on the fluorescence rate at ≅15%–20% and to reach bleaching times of the order of 70 s or longer (43).

Fluorescence lifetime

A PCI-Board for time-correlated single-photon counting (TCSPC) (Time Harp 200, PicoQuant, Berlin, Germany) was employed to measure times of arrival (with respect to the laser pulse) of photons collected from single proteins by the SPAD module. By simultaneously collecting the fluorescence rate (at 0.1-ms sampling time), we could also check that the duration of lifetime measurements (typically ≅10 s) was less than the bleaching time for each observed protein. The count for each single-molecule lifetime measurement was typically at least 100,000 photons at the excitation intensity ≅10 kW/cm^2. The full half-height width of the intensity response function is ≅300 ps (43).

Fluorescence polarization

The fluorescence signal was split by a polarizing cube beam splitter and sent to the two SPAD modules. The optical setup has different responses, $S_\parallel$ and $S_\perp$, to the light polarization parallel and perpendicular to the exciting one, and this affects the polarization measurements through the factor $G = S_\perp/S_\parallel$ (46) for the setup used here, $G \cong 0.9$. The measurement of the average fluorescence signal with polarization parallel, $\langle I_\parallel \rangle$, and perpendicular, $\langle I_\perp \rangle$, to the excitation polarization allowed the computation of the fluorescence polarization $\langle P \rangle = (\langle I_\parallel \rangle - G\langle I_\perp \rangle)/(\langle I_\parallel \rangle + G\langle I_\perp \rangle)$ (47). The average of the fluorescence signals from each single protein was computed on ~10 s at the excitation intensity ≅10 kW/cm^2.

RESULTS AND DISCUSSION

Spectroscopic characterization

We measured the molecular brightness, fluorescence bleaching time, and excited state lifetime of ~150 single-GFPmut2 proteins embedded in trehalose-water matrixes of different sugar content, dehydrated for 30 min at 60°C after spin coating. Recall that traces of residual water are present even in extremely dry samples (21–24). A typical image of a spin-coated trehalose solution (35% w/w) is shown in Fig. 1 A.
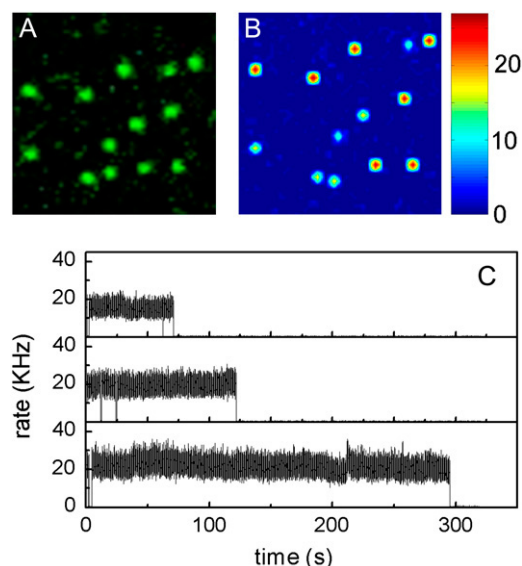
FIGURE 1 (A) 3.5 × 3.5 μm (70-nm pixel size, dwell time 1 ms) of single-GFP molecules obtained by spin coating trehalose-GFP solutions on glass slides. (B) contour plot of the field of view reported in A, showing different values of the brightness, ε, for spots that were proved to correspond to single-GFP molecules according to the single-step bleaching behavior (see text). The unit on the color bar is kHz. (C) Fluorescence intensity (adjacent averaging on 10 points) versus time of three single-GFP molecules out of those visible in the field of view reported in A and B.
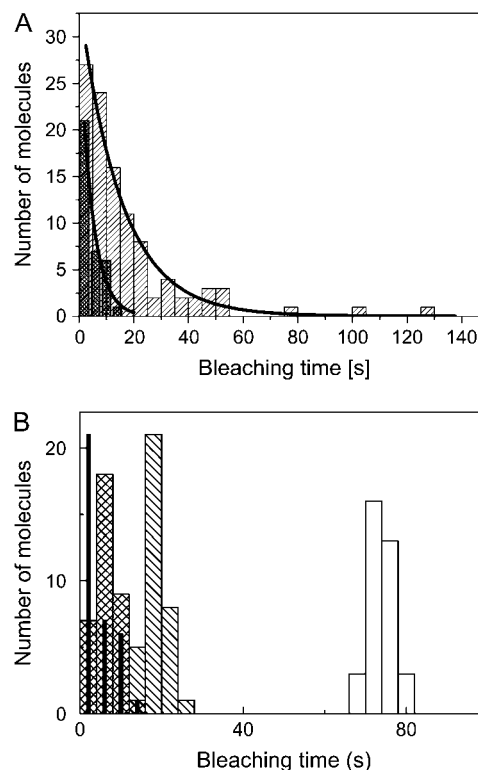

FIGURE 2 (A) distributions of the single-molecule bleaching time of GFP (spin coated on clean glass, equivalent, in terms of spectroscopic parameters, to one of the protein families reported hereafter) under single- (*sparse patterned bars*) and two-photon (*dense patterned bars*) excitation, corrected for the blinking dark times. One-photon excitation: excitation wavelength = 488 nm, excitation intensity 40 kW/cm^2, emission filter 515 ± 15 nm. TPE: excitation wavelength = 860 nm, I_{exc} = 30 kW/cm^2, emission filter 515 ± 15 nm. The solid lines are the best fit exponential function to the data: relaxation times are 4.6 ± 0.8 s and 15 ± 1 s for the one- and two-photon excitation, respectively. (B) Histogram of the absolute bleaching time versus the excitation intensity, 30 (*crosses bars*), 20 (*slant dashed bars*), and 10 kW/cm^2 (*white bars*). The thin black bars represent the distribution of the GFP bleaching times corrected for the total duration of the dark blinking times (I_{exc} = 30 kW/cm^2).

The presence of spots exhibiting different fluorescence brightness (photons collected per unit time) is evidenced in the contour plots shown in panel B, and the different bleaching times, T_B, are shown in panel C. On the selected single-molecule spots we reach, at I_{exc} = 10 kW/cm^2, a signal/noise ratio ≅ 5.

Under one- and two-photon excitation, at high laser intensity the distribution of bleaching times measured on GFP is exponential (Fig. 2 A, and Supplementary Material). However, both the average value (48) and the form of the distribution of the bleaching times depend on the excitation intensity and the excitation mode (49,50). In fact, under TPE at low laser intensity (below ~20 kW/cm^2), peaked distributions of T_B, well described by Gaussian functions, are found for GFP on clean glasses (Fig. 2 B) and in trehalose matrices (see below). Interestingly, the shape of the distribution changes from Gaussian to exponential, when T_B values are corrected for the blinking dark times (Fig. 2 B and Supplementary Material); such correction causing a decrease of only 4% ± 0.6% of the average bleaching times at the lowest excitation intensity (≅10 kW/cm^2). The origin of such behavior is not yet well understood. It has been suggested (44) that TPE thermal loading of the matrix induced by the laser intensities contributes to determining the T_B values.

To characterize, with good statistics, the protein fluorescence dynamics through the set of parameters that we report, we needed to observe fluorescing proteins for long times. Accordingly, since the bleaching time is an inverse function

of the excitation intensity (48), we have been forced to use low excitation intensities (≅10 kW/cm^2), thus obtaining Gaussian distributions of bleaching times, T_B (see Fig. 3). In any case, since T_B values must depend on the nanoenvironment of the molecule, the three different distributions, reported hereafter (Fig. 3), must stem from a different matrix nanostructure, which, trusting the thermal origin of the observed bleaching behaviors, might correspond to different thermal conductivities of the protein surroundings.

Fluorescence bleaching time versus trehalose concentration

At the excitation intensity I_{exc} ≅ 10 kW/cm^2 (corresponding to ~25 μW excitation power), a single-GFP molecule spin coated on a glass coverslip has, in the absence of trehalose,
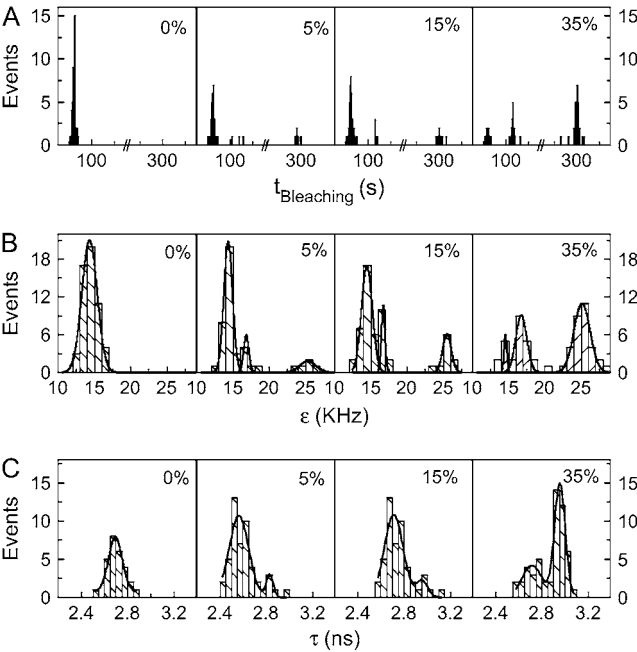
FIGURE 3 Spectroscopic characterization of single-GFP molecules spin coated on glass coverslips. The trehalose concentration of the GFP-trehalose solutions (w of trehalose/w of solution %) is reported in the panels. (A) histograms of the bleaching time values. (B) histograms of fluorescence brightness values. (C) Histograms of the excited state lifetime values.

TABLE 1 Spectroscopy parameters of single-GFPmut2 proteins trapped in 35% of trehalose under 10 kWcm^{-2} excitation intensity
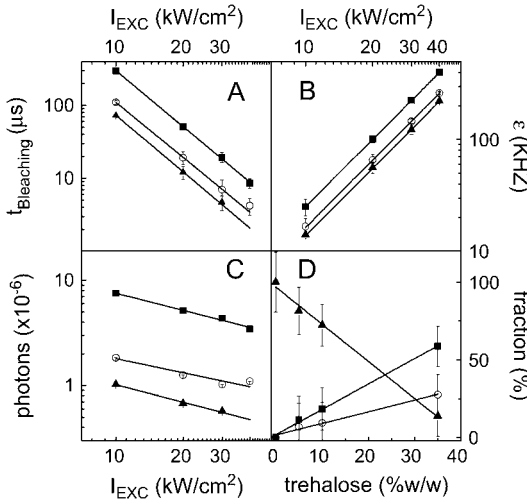
	Family "H"	Family "I"	Family "L" and Silica Gel Family
Bleaching Time T_B [s]	300 ± 7	110 ± 6	73 ± 2
Brightness [kHz]	25 ± 2	17 ± 1	15 ± 1
Lifetime [ns]	3.0 ± 0.1	–	2.7 ± 0.1

Values are reported together with their standard error.

shown in the Supplementary Material, the presence of the three families of proteins can also be inferred from a multi-exponential analysis of the distributions of the single-photon bleaching times, although it is far more evident from the peaked two-photon bleaching time distribution.

Molecular brightness versus trehalose concentration

In the absence of trehalose at $I_{exc} = 10$ kW/cm^2, the molecular brightness of single-GFPmut2 spin-coated molecules is found to be $\varepsilon = 15 \pm 1$ kHz, in good agreement with the value found in silica gels (43) whereas, in the presence of the sugar, some proteins display higher brightness. In particular, as shown in Table 1 even in sample prepared from 5% trehalose solutions, three populations—characterized by

an average bleaching time $T_B = 73 \pm 2$ s, in good agreement with the value found in silica gels under the same excitation/detection conditions (43). This suggests that the interaction of the protein with the coverslip surface does not sizably affect the fluorescence stability. Already in the sample prepared by spin-coating solutions of the lowest trehalose concentration (5% w/w), some molecules display much longer bleaching times, $T_B \cong 300 \pm 7$ s and $T_B \cong 110 \pm 6$ s (Table 1). The presence of three distinct GFPmut2 families, characterized by three values of bleaching times, is visualized by the histogram analysis over ~100 molecules, shown in Fig. 3 A. Increasing trehalose concentration makes the relative population of the three families progressively vary, whereas the mean bleaching time, for each family, remains unaltered. In a sample prepared by spin-coating solutions of 35% w/w trehalose concentration, more than half (~55%) of the single proteins investigated have the longest bleaching time, $T_B \cong 300$ s. As Fig. 4 A shows, the bleaching time decreases by increasing the excitation power with a 2.5 power law, as usually found for TPE (43).

Fluorescence bleaching is sizably affected by the excitation mode. Under single-photon excitation the distribution of bleaching times is exponential or multiexponential, whereas under TPE, at the very low excitation intensities used here, peaked distributions of the bleaching time are found (Supplementary Material). We have verified that for GFPmut2 embedded in trehalose-water, the bleaching time distributions under single-photon excitation remain exponential. As

FIGURE 4 Spectroscopic parameters for the three classes of GFPmut2 proteins in 35% w/w trehalose samples. The symbols refer to the most stable (*solid squares*), intermediate (*open circles*), and less stable (*solid up triangles*) molecules. (A) Bleaching time versus the excitation intensity I_{EXC} for the three different groups of GFP molecules embedded in trehalose samples at 35% w/w. Solid lines are best fit to a power law $\cong I_{EXC}^{-2.5}$. (B) Molecular brightness versus I_{EXC}. Solid lines are best fit to a power law $\cong I_{EXC}^{2}$. (C) Total number of photons emitted by single proteins before bleaching versus I_{EXC}. Solid lines are best fit to a power law $\cong I_{EXC}^{-0.5}$. (D) Fraction of the three populations versus the trehalose concentration. Solid lines are linear best fit to the data. Bars indicate the standard deviations of the data.

$\varepsilon \cong 15$ kHz, 17 kHz, and 25 kHz—are present. By increasing trehalose concentration in the spin-coated samples, the average values of ε for the three families remain unaffected, whereas the relative weight of the highest brightness component increases (Fig. 3 *B*). Several images have been taken at increasing excitation intensity from $I_{exc} = 10$–100 kW/cm^2; as expected for TPE processes, the fluorescence rates for the three populations (Fig. 4 *B*) exhibit a quadratic dependence upon the excitation intensity. Furthermore, measurements at increasing excitation intensity enabled us to have a good resolution for the two low brightness populations.

Fluorescence lifetime versus trehalose concentration

In the absence of trehalose, the fluorescence decay of spin-coated single-GFPmut2 molecules is well described by a single-exponential function whose average lifetime is $\tau \cong 2.7 \pm 0.2$ ns. As Fig. 3 *C* shows, the presence of trehalose causes a progressive broadening of the lifetime distribution, which, at 35% w/w, becomes clearly bimodal, exhibiting a second peak at $\tau \cong 3 \pm 0.2$ ns (Table 1).

Hydration effects

The effect of the sample hydration on the GFP photophysical parameters has been investigated at the highest sugar concentration (35% w/w). Samples were dried for 30 min at 60°C and then set on the microscope stage where they rapidly took up water, reaching equilibrium with the surrounding moisture (15% humidity) (19,20). The fluorescence emission of ~20 different GFPmut2 molecules has been recorded at 30-min sampling time while varying the humidity in the sample atmosphere. Two different experiments have been performed, which enabled us to follow the effects of either samples' hydration or dehydration, as described in detail in the following.

GFPmut2 emission versus the sample dehydration

In a first experiment, the samples, previously dried at 60°C for 30 min, were placed in a sealed chamber at room temperature and further dried in the presence of a constant nitrogen flux. The fluorescence emission was monitored for a total of 210 min (Fig. 5 *A*) while slowly lowering the chamber humidity down to ~5%. For these experiments we have adopted an interleaved excitation mode in which each protein was continuously excited and observed for a time stretch much smaller than the average bleaching time and left otherwise in the dark. In this way, we enhanced the protein photostability (40,44) while observing the long time evolution of protein photodynamics. During the drying, the
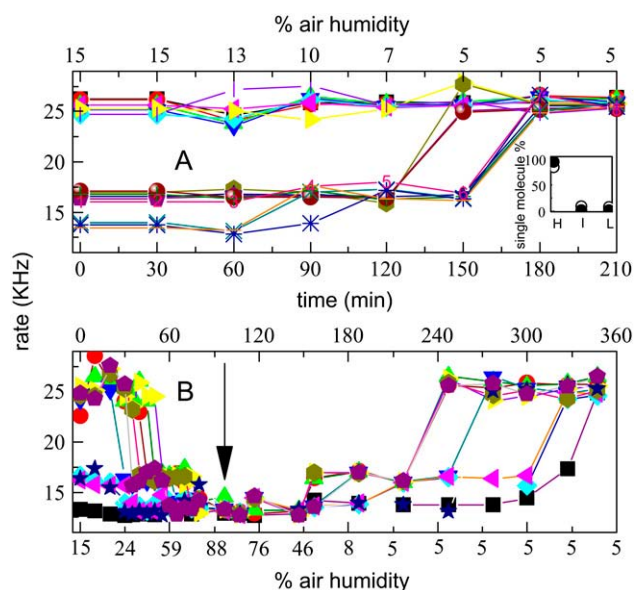

FIGURE 5 Transitions between GFP populations while changing the water content of the sample. (*A*) Fluorescence rate of single-GFPmut2 proteins versus time during gel (35% w/w trehalose content) dehydration under dry nitrogen flux. The proteins, mostly in the lowest brightness family (L) at moderate water content, undergo transition to the intermediate (I) and highest (H) brightness families at decreasing water content. (*B*) Fluorescence emission of single-GFP proteins versus time in an initially dehydrated (60°C for 30 min) 35% w/w trehalose sample. At time = 0 min the sample was incubated in water saturated air. At time $\cong$90 min (*vertical arrow* in the plot) a dry nitrogen flux was allowed to reach the sample while continuously monitoring the single-GFP proteins fluorescence emission for the following 260 min. (*Inset*) percentage of the three populations of proteins (H, I, and L), discriminated according to the molecular brightness and detected on trehalose samples that have been dehydrated at 60°C for 60 (*open circles*) and 90 (*solid squares*) min.

highest brightness proteins maintained constant fluorescence emission rate, whereas the lower brightness ones gradually underwent transition to the brightest state. Such a transition was confirmed by the population distribution measured when increasing the drying time at 60°C from 30 to 60 and 90 min, as shown in the inset of Fig. 5 *A*. Indeed, after 90 min dehydration at 60°C, the brightest population is $\cong$95% of the molecules analyzed, whereas the lowest brightness component almost disappears.

Hydration-dehydration cycles

In this experiment, trehalose-containing samples were first hydrated by putting them in the presence of ~94% humidity for 100 min and then dried by fluxing dry nitrogen. Fig. 5 *B* shows the hydration dependence of single-protein fluorescence brightness; as evident by increasing the sample hydration, the brightest proteins undergo a transition to the dimmest family, which at ~94% humidity contains all the proteins under analysis. At variance, decreasing the sample hydration by flushing dry nitrogen makes the overall sample

harden and the proteins recover their original brightness distribution.

To detect the transitions of the protein among different states while changing the ambient humidity, we also followed the fluorescence emission of ∼40 proteins versus time at 1-ms resolution. Two temporal traces are reported in Fig. 6, *A* and *B*, the first showing a transition from the brightest to the intermediate state and the second a transition from the intermediate to the dimmest states. The existence of two definite fluorescence levels is also proved by the histogram analysis of the fluorescence traces (Fig. 6, *E* and *F*), which is well described by the sum of two Gaussian components.

As mentioned in the Material and Methods section, the fluorescence properties of the GFPmut2 protein depend on proton ejection and rebinding to the chromophore. Fluorescence blinking, due to the anionic-zwitterionic state transition of the chromophore, occurs in the second time range and has been resolved in the experiment reported here (Fig. 1 *C*). A faster (10–100 μs) fluorescence dynamics in GFP is largely determined by the neutral-anionic (N-A) switching which occurs via some tiny rearrangement in the chromophore pocket (Thr-203) and on the protein surface (His-148) (52) and is likely to depend on hydration.

When following the fluorescence dynamics at 10-μs time resolution, we find that the anionic-neutral switching rate is

remarkably different for the proteins belonging to the three different families (see Supplementary Material). In particular the N-A switching rate is >30 events/min for the brightest family, between 10 and 30 events/min for the intermediate family, and <10 events/min for the dimmest family. Therefore the N-A switching rate could be taken as a parameter, in addition to brightness and bleaching time, for the characterization of the type of protein family. All together, these results indicate that the internal dynamics, i.e., protonation-deprotonation of the chromophore, which is closely related to the protein environment through a hydrogen-bonding network, is also affected by the hydration and trehalose content. However, it must be noted that the observed increase of the N-A switching rate for the dimmest family with respect to the brightest one does not alone account for the differences in the molecular brightness (Fig. 3 *B*) sampled at 1-ms time resolution.

Fluorescence polarization measurements

To better understand the origin of the above three GFPmut2 families, we performed fluorescence polarization, P, measurements on 35% trehalose samples, removing the quarter wavelength plate that randomizes the excitation polarization. Single-molecule fluorescence polarizations fall into three distinct intervals, as shown in Fig. 7, *A–C*, stemming from the three above classes of GFP molecules. In particular, the anisotropy distribution is very narrow for the brightest class (peaked at ∼0.6), and it broadens for the intermediate (peaked at 0.5) and for the lowest brightness class (peaked at ∼0). Although for a more quantitative analysis the depolarization induced by the microscope objective should be taken into account (53), the observed distributions of P shows that the brightest GFP molecules explore fewer degrees of freedom.

The spectroscopic parameters in Fig. 3 and their power dependence (Fig. 4) evidence that three populations of GFPmut2 molecules can be resolved. In particular, the bleaching time appears to be the property most sensitive to the local protein environment since it shows, in the presence of trehalose, three quite distinct values spanning a more than fourfold interval. The molecular brightness, although showing minor changes, can also be grouped into three major components, well split even at $I_{\mathrm{EXC}} \cong 10\ \mathrm{kW/cm}^2$ (Fig. 4 *B*). The excited state lifetime, which shows only two distinct values, 2.7 ns and 3 ns (with a standard deviation of ∼0.1 ns), is less sensitive to the protein environment. However, in view of the three components observed for the bleaching time and the molecular brightness, we think it is likely that the two excited state lifetimes actually correspond to three not fully resolved populations of proteins.

The distinction into three populations that can be clearly made according to T_{B} and ε appears even more evident when considering the total number, N_{TOT}, of photons collected from a single-GFP molecule before bleaching, given by $T_{\mathrm{B}} \times \varepsilon$ and
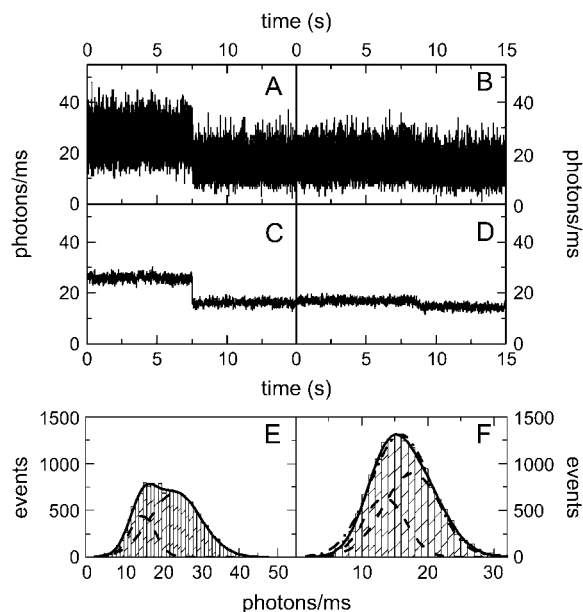
FIGURE 6   Transitions of single GFP between families of different brightness observed by following the fluorescence emission versus time upon hydrating the samples. (*A* and *B*) fluorescence trace collected at 1-ms time resolution. (*C* and *D*) The same fluorescence traces shown in *A* and *B* averaged at 50-ms sampling time. (*E* and *F*) Histograms of the fluorescence signals reported in *A* and *B*, respectively. The lines are Gaussian fits to the histogram. (*E*, *solid line*) two-component Gaussian fit; (*dashed lines*) single components of the fit. (*F*) Dot-dashed line is a single-Gaussian fit to the histogram; solid and dashed lines are the two component Gaussian best fit curve and the two Gaussian fit components.
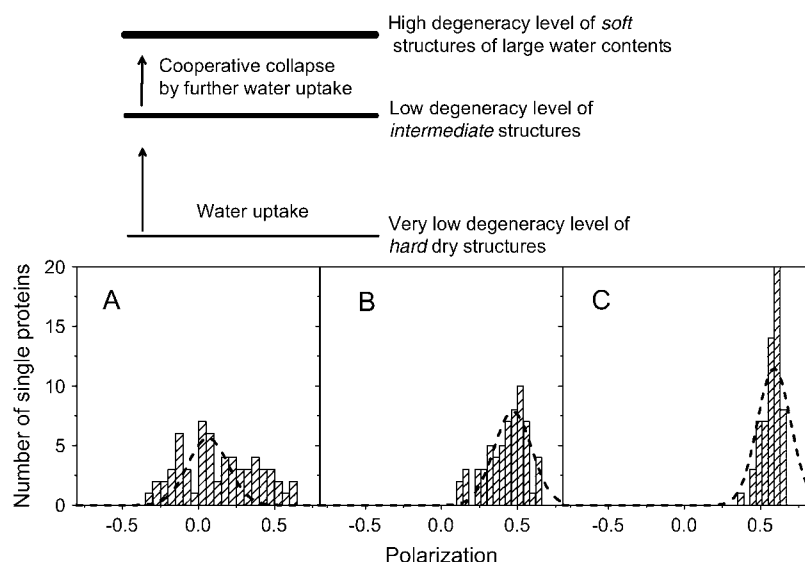
FIGURE 7 Fluorescence polarization of single-GFP proteins in 35% trehalose samples. (*A–C*) Histograms of the fluorescence polarization values for the GFP proteins belonging to the L, I, and H classes, respectively. The dotted lines show the shot noise contribution to the width of the polarization distribution (58). A scheme of the transition among different substates, which also consider the degeneracy according to the fluorescence brightness and polarization data, is also sketched.

shown in Fig. 4 *C* versus the excitation intensity. In particular, at 10 kW/cm^2, the number of photons emitted by the brightest molecules is about one order of magnitude larger than the one in the dimmest state. We also note that N_{TOT} is actually decreasing versus the beam excitation intensity as $I_{EXC}^{-0.5}$ (Fig. 4 *C*) as expected since the bleaching time decreases as $I_{EXC}^{-2.5}$ (Fig. 4 *A*) while the brightness increases as I_{EXC}^2 (Fig. 4 *B*).

From now on, we shall refer to the above characterized three families of GFPmut2 as ''L'' (short T_B), ''I'' (intermediate T_B), and ''H'' (long T_B). As shown, such families exhibit a tight correlation between all the spectroscopic properties examined; indeed, molecules with longer T_B ($\cong$300 s) also display enhanced brightness $\varepsilon \cong 25$ kHz and longer lifetime $\tau \cong 3$ ns, whereas molecules that bleach after only 70 s also have a lower brightness, $\varepsilon \cong 15$ kHz, and shorter lifetime, $\tau \cong 2.7$ ns.

Fig. 4 shows the population of each class, evaluated from their relative weight in the histogram of bleaching times (Fig. 3), measured in samples prepared from solutions of different sugar content, dehydrated for 30 min at 60°C. As evident from Fig. 4, the relative populations scale linearly with the solution's trehalose concentration; indeed, samples richer in trehalose are richer in more photostable molecules. Similar results are also obtained from the analysis of molecular brightness.

All the fluorescence parameters relative to the ''L class'' GFP molecules fall very close to the ones found either in the absence of trehalose or in silica gels (43); this suggests that L class molecules barely ''feel'' trehalose effects. In contrast, class H proteins seem to be the ones that feel the presence of trehalose molecules the most, as evidenced by all the fluorescence parameters measured. In a previous work (28) it was suggested that the photobleaching time distributions measured in individual metal-free porphyrin cytochrome *c* and Zn porphyrin cytochrome *c* embedded in trehalose-containing matrixes were indicative of the fact that the

trehalose glass restricts the accessibility of the fluorescent molecules to oxygen. We believe that our results, which evidence the presence of different and interconverting single-molecule populations exhibiting different brightness, bleaching times, polarization anisotropy, and broadening of the lifetime distribution, could hardly be rationalized in terms of the sample's oxygen accessibility.

We suggest that the three different classes of GFPmut2 molecules originate from protein-sugar-water structures (21, 25), which, as shown by the whole set of data reported, harden by lowering the water molecules involved. In particular, the brightness increases for the ''H class'' (hard structures) is in agreement with what is known for the GFP chromophore quantum yield (54). Our suggestion is confirmed by the behavior observed when performing hydration-dehydration cycles; indeed, at the highest humidity all the proteins fall into the L class, whereas at the highest drought they all fall into the H class. It is noteworthy that, in view of the fact that the local humidity at the protein surroundings does, most likely, not ''follow in phase'' the chamber humidity, a hysteresis is observed in the dehydration-hydration cycles. The above observations indicate that each protein may jump between different classes, thus implying thermal equilibrium among the protein-trehalose-water structures, which from now on we shall assume to reflect protein-solvent conformational substates (55). In this respect, our data suggest that both the observed ''I'' and ''H'' classes correspond to low probability substates in aqueous solutions, whose likelihood is largely increased by hardening of the structure.

As Fig. 6 *A* shows, the transition of a single protein, initially belonging to the brightest (H) family, to an intermediate (I) emission level is clearly discernible even at a 1-ms time resolution. Averaging the fluorescence emission over 50 ms acquisition time enables us to observe an even clearer transition (Fig. 6 *C*), which appears to be sharp with no intermediate fluorescence emission levels. The histogram of the

fluorescence rates (at a 1-ms sampling time) for this transition, which can be fit to a double-component Gaussian function, clearly evidences the presence of two maxima (Fig. 6 *E*). The average rates (16 ± 1.8 kHz and 26 ± 2 kHz) correspond to the values observed for the intermediate and the brightest protein class. At variance, the transition of a single-GFP protein from the intermediate (I) to the dimmest (L) proteins class is not clearly discernible at a 1-ms resolution (Fig. 6 *B*). For unequivocally detecting such a transition, we needed to average the fluorescence photons over a 50-ms acquisition time (Fig. 6 *D*). Nevertheless, the transition can still be detected on the high time resolution data from a histogram analysis (Fig. 6 *F*); indeed, the asymmetric curve shown in Fig. 6 *F* can be fit to a two-component Gaussian function with average rates (14.4 ± 1.6 kHz and 17.0 ± 1.8 kHz) corresponding to the emission of the dimmest and intermediate brightness classes. A single-component Gaussian (*dot-dashed line* in Fig. 6 *F*) does not adequately fit the histogram.

As is the well known, supercooled fluids and nonsolid glasses, near the glass transition, exhibit locally spatial heterogeneous dynamics (56 and references therein). Based on our observations, we suggest the three families of trehalose-water-protein structures (21,25) detected (one very bright (25 kHz) and two of slightly different low brightness (15 and 17 kHz)) undergo (according to the data shown in Fig. 6, *C* and *D*) sharp, sudden reorganization within the glass-forming trehalose-water matrix, according to the scheme in Fig. 7. Indeed, sequential uptake ↔ release of very few water molecules may cause the H⇌I and I⇌L transition, the latter being soft structures which are barely affected by the addition of further water molecules. The difference in the degeneracy among protein-trehalose-water structures of different hardness in the scheme (Fig. 7) can be related to the large disparity in the width of the polarization anisotropy histograms for the three protein families.

Hochstrasser and co-workers (28) in their single-molecule study performed on metal-free porphyrin cytochrome *c* and Zn porphyrin cytochrome *c* in low concentration (1%) trehalose glasses reported that the protein undergoes some angular jumps characteristic of hindered motions that are likely to occur in solvent/solute cavities with size and hydrogen network structures determined by the trehalose/water content ratio. In full agreement, the polarization measurements reported here (Fig. 7) indicate that some restricted motions are occurring for subpopulations of the protein ensemble that correspond to lower brightness and limited photostability and might be related to differing hydrogen-bonding networks with the ''solvent''.

CONCLUSIONS

The reported results are in full agreement, at the single-molecule level, with the suggestion (21,25) that proteins embedded in water-trehalose matrixes are confined within a hydrogen-bonds network whose rigidity increases by lowering the hydration level. Such a network anchors the protein surface to the surrounding water-sugar matrix and couples the internal degrees of freedom of the protein to those of the surroundings. Furthermore, measurements performed at different hydration levels evidence how the rigidity of the protein-water-trehalose structures is not homogeneous over the whole sample during the drying process. Three different, interconverting protein families, corresponding to protein-solvent conformational substates of three different rigidity levels, are simultaneously present. In particular

1) In wet samples, the population distribution is almost fully displaced toward soft substates.
2) In samples of intermediate water content, all three substates are present.
3) In the driest samples, the population distribution is almost fully displaced toward the hard substates.

Furthermore, the presence of only a single very bright and two slightly different low brightness protein-solvent conformational substates is indicative of the cooperative collapse of the hard trehalose-water-protein structures.

Heterogeneous hardening of the trehalose-water matrix has been invoked (23) to rationalize the finding (19) that, in MbCO embedded in trehalose-water matrixes, the thermal interconversion among taxonomic A substates (in the range 263–323 K) is progressively hindered when the sample's residual water content was decreased from very humid to very dry samples. Since the distribution of conformational substates at a given temperature is an equilibrium property, the observed progressive reduction of interconversion in nonsolid matrixes (during sample dehydration) suggested such a process is not related to an increasing viscosity but rather to a spatially heterogeneous stiffening of the trehalose matrix. The data reported here support the suggestion that during the drying of the sample only a fraction of proteins molecules is allowed to fluctuate among different conformational substates; whereas for the remaining fraction (which increases by decreasing the water content) the fluctuations, driving the crossing of the energy barriers, can be hindered. Analogous spatially heterogeneous dynamics has also been invoked to rationalize the progressive hindering of the conformationally gated QA → QB electron transfer in reaction centers from *Rhodobacter sphaeroides* embedded in trehalose matrixes of decreasing residual water (16).

We believe that these data contribute to the understanding, at the single molecule level, of the well-known heterogeneous structure and dynamics in concentrated carbohydrate-water systems (57) and more generally in supercooled fluids (56 and references therein).

SUPPLEMENTARY MATERIAL

An online supplement to this article can be found by visiting BJ Online at http://www.biophysj.org.

REFERENCES

1. Crowe, L. M. 2002. Lesson from nature: a role of sugars in anhydrobiosis. *Comp. Biochem. Physiol. A.* 132:505–513.

2. Bianchi, G., A. Gamba, C. Murellie, F. Salamini, and D. Bartels. 1991. Novel carbohydrate metabolism in the resurrection plant. *Craterostigma Plantagineum. Plant J.* 1:355–359.

3. Uritani, M., M. Takai, and K. Yoshinaga. 1995. Protective effect of disaccharides on restriction endonucleases during drying under vacuum. *J. Biochem. (Tokyo).* 117:774–779.

4. Panek, A. D. 1995. Trehalose metabolism—new horizons in technological applications. *Braz. J. Med. Biol. Res.* 28:169–181.

5. Crowe, J. H., and L. M. Crowe. 1984. Preservation of membranes in anhydrobiotic organisms: the role of trehalose. *Science.* 223:701–703.

6. Crowe, J. H., L. M. Crowe, and S. A. Jackson. 1983. Preservation of structural and functional activity in lyophilized sarcoplasmic reticulum. *Arch. Biochem. Biophys.* 220:615–617.

7. Crowe, L. M., and J. H. Crowe. 1995. Freeze-dried liposomes. *In* Liposomes, New Systems and New Trends in Their Applications. F. Puisieux, P. Covreur, L. Delattre, and J. P. Devissaguet, editors. Editions de Santè, Paris. 237–272.

8. Hagen, S. J., J. Hofrichter, and W. A. Eaton. 1995. Protein reaction kinetics in a room temperature glass. *Science.* 269:959–962.

9. Gottfried, D. S., E. S. Peterson, A. G. Sheikh, J. Wang, M. Yang, and J. M. Friedman. 1996. Evidence for damped hemoglobin dynamics in a room temperature glass. *J. Phys. Chem.* 100:12034–12042.

10. Cordone, L., P. Galajda, E. Vitrano, A. Gassmann, A. Ostermann, and F. Parak. 1998. A reduction of protein specific motions in co-ligated myoglobin embedded in a trehalose glass. *Eur. Biophys. J.* 27:173–176.

11. Cordone, L., M. Ferrand, E. Vitrano, and G. Zaccai. 1999. Harmonic behavior of trehalose-coated carbon-monoxy-myoglobin at high temperature. *Biophys. J.* 76:1043–1047.

12. Rector, D., J. Jiang, M. A. Berg, and M. D. Fayer. 2001. Effects of solvent viscosity on protein dynamics: infrared vibrational echo experiments and theory. *J. Phys. Chem. B.* 105:1081–1092.

13. Schlichter, J., J. Friedrich, L. Herenyi, and J. Fidy. 2001. Trehalose effect on low temperature protein dynamics: fluctuation and relaxation phenomena. *Biophys. J.* 80:2011–2017.

14. Ponkratov, V. V., J. Friedrich, and J. M. Vanderkooi. 2002. Solvent effect on conformational dynamics of proteins: cytochrome *c* in a dried trehalose film. *J. Chem. Phys.* 117:4594–4601.

15. Palazzo, G., A. Mallardi, A. Hochkoeppler, L. Cordone, and G. Venturoli. 2002. Electron transfer in photosynthetic reaction center embedded in trehalose glasses: trapping of conformational substates at room temperature. *Biophys. J.* 82:558–568.

16. Francia, F., G. Palazzo, A. Mallardi, L. Cordone, and G. Venturoli. 2003. Residual water modulates Q_A^- to Q_B electron transfer in bacterial reaction centers embedded in trehalose amorphous matrixes. *Biophys. J.* 85:2760–2775.

17. Francia, F., G. Palazzo, A. Mallardi, L. Cordone, and G. Venturoli. 2004. Probing light-induced conformational transitions in bacterial photosynthetic reaction centers embedded in trehalose-water amorphous matrixes. *Biochim. Biophys. Acta.* 1658:50–57.

18. Cottone, G., L. Cordone, and G. Ciccotti. 2001. Molecular dynamics simulation of carboxy-myoglobin embedded in a trehalose-water matrix. *Biophys. J.* 80:931–938.

19. Librizzi, F., E. Vitrano, and L. Cordone. 1999. Inhibition of A substates interconversion in trehalose coated carbonmonoxymyoglobin. *In* Biological Physics. H. Frauenfelder, G. Hummer, and R. Garcia, editors. AIP American Institute of Physics, Melville, NY. 132–138.

20. Librizzi, F., C. Viappiani, S. Abbruzzetti, and L. Cordone. 2002. Residual water modulates the dynamics of the protein and of the external matrix in "trehalose coated" MbCO: an infrared and flash photolysis study. *J. Chem. Phys.* 116:1193–1200.

21. Giuffrida, S., G. Cottone, F. Librizzi, and L. Cordone. 2003. Coupling between the thermal evolution of the heme pocket and the external matrix structure in trehalose coated carboxymyoglobin. *J. Phys. Chem. B.* 107:13211–13217.

22. Giuffrida, S., G. Cottone, and L. Cordone. 2004. Structure-dynamics coupling between protein and external matrix in sucrose-coated and in trehalose-coated MbCO: an FTIR study. *J. Phys. Chem. B.* 108:15415–15421.

23. Cordone, L., G. Cottone, S. Giuffrida, G. Palazzo, G. Venturoli, and C. Viappiani. 2005. Internal dynamics and protein-matrix coupling in trehalose coated proteins. *Biochim. Biophys. Acta.* 1749:252–281.

24. Giuffrida, S., G. Cottone, and L. Cordone. 2006. Role of solvent on protein-matrix coupling in MbCO embedded in water-saccharide systems: an FTIR study. *Biophys. J.* 91:968–980.

25. Cottone, G., G. Ciccotti, and L. Cordone. 2002. Protein-trehalose-water structures in trehalose coated carboxy-myoglobin. *J. Chem. Phys.* 117:9862–9866.

26. Cottone, G., S. Giuffrida, G. Ciccotti, and L. Cordone. 2005. Molecular dynamics simulation of sucrose- and trehalose-coated carboxy-myoglobin. *Proteins.* 59:291–302.

27. Abbruzzetti, S., S. Giuffrida, S. Sottini, C. Viappiani, and L. Cordone. 2005. Light-induced protein-matrix uncoupling and protein relaxation in dry samples of trehalose-coated MbCO at room temperature. *Cell Biochem. Biophys.* 43:431–438.

28. Mei, E., J. Tang, J. M. Vanderkooi, and J. M. Hochstrasser. 2003. Motions of single molecules and proteins in trehalose glass. *J. Am. Chem. Soc.* 125:2730–2735.

29. Cormack, B. P., R. H. Valdivia, and S. Falkow. 1996. FACS-optimized mutants of the green fluorescent protein (GFP). *Gene.* 173:33–38.

30. Cubitt, A. B., R. Heim, S. R. Adams, A. E. Boyd, L. A. Gross, and R. Y. Tsien. 1995. Understanding, improving and using green fluorescent proteins. *Trends Biochem. Sci.* 20:448–455.

31. Bokman, S. H., and W. W. Ward. 1981. Renaturation of Aequorea green-fluorescent protein. *Biochem. Biophys. Res. Commun.* 101:1372–1380.

32. Ward, W. W., C. W. Cody, R. C. Hart, and M. J. Cormier. 1980. Spectrophotometric identity of the energy transfer chromophores in Renilla and Aequorea green-fluorescent proteins. *Photochem. Photobiol.* 31:611–615.

33. Ward, W. W., and S. H. Bokman. 1982. Reversible denaturation of Aequorea green-fluorescent protein: physical separation and characterization of the renatured protein. *Biochemistry.* 21:4535–4540.

34. Campanini, B., S. Bologna, F. Cannone, G. Chirico, A. Mozzarelli, and S. Bettati. 2005. Unfolding of green fluorescent protein mut2 in wet nanoporous silica gels. *Protein Sci.* 14:1125–1133.

35. Ezaz-Nikpay, K., K. Uchino, R. E. Lerner, and G. L. Verdine. 1994. Construction of an overproduction vector containing the novel srp (sterically repressed) promoter. *Protein Sci.* 3:132–138.

36. Cormack, B. P., R. H. Valdivia, and S. Falkow. 1996. FACS-optimized mutants of the green fluorescent protein (GFP). *Gene.* 173:33–38.

37. Chirico, G., F. Cannone, S. Beretta, A. Diaspro, B. Campanini, S. Bettati, R. Ruotolo, and A. Mozzarelli. 2002. Dynamics of green fluorescent protein mutant2 in solution, on spin-coated glasses, and encapsulated in wet silica gels. *Protein Sci.* 11:1152–1161.

38. Cannone, F., G. Chirico, G. Baldini, and A. Diaspro. 2003. Measurement of the laser pulse width on the microscope objective plane by modulated autocorrelation method. *J. Microsc.* 210:149–157.

39. Malengo, G., R. Milani, F. Cannone, S. Krol, A. Diaspro, and G. Chirico. 2004. High sensitivity optical microscope for single molecule spectroscopy studies. *Rev. Sci. Instrum.* 75:2746–2751.

40. Cannone, F., S. Bologna, B. Campanini, A. Diaspro, S. Bettati, A. Mozzarelli, and G. Chirico. 2005. Tracking unfolding and refolding of single GFPmut2 molecules. *Biophys. J.* 89:2033–2045.

41. Chirico, G., F. Cannone, S. Beretta, A. Diaspro, B. Campanini, S. Bettati, R. Ruotolo, and A. Mozzarelli. 2002. Dynamics of green fluorescent protein mutant2 in solution, on spin-coated glasses, and encapsulated in wet silica gels. *Protein Sci.* 11:1152–1161.

42. Chirico, G., F. Cannone, and A. Diaspro. 2003. Single molecule photodynamics by means of one- and two-photon approach. *J. Phys. D: Appl. Phys.* 36:1682–1688.

43. Cannone, F., M. Caccia, S. Bologna, A. Diaspro, and G. Chirico. 2004. Single molecule spectroscopic characterization of GFP-MUT2 mutant for two-photon microscopy applications. *Microsc. Res. Tech.* 65:186–193.

44. Chirico, G., F. Cannone, G. Baldini, and A. Diaspro. 2003. Two-photon thermal bleaching of single fluorescent molecules. *Biophys. J.* 84:588–598.

45. Zondervan, R., F. Kulzer, M. A. Kol'chenko, and M. Orrit. 2004. Photobleaching of rhodamine 6G in poly(vinyl alcohol) at the ensemble and single-molecule levels. *J. Phys. Chem. A.* 108:1657–1665.

46. Collini, M., L. D'Alfonso, A. Oldani, L. Cellai, C. Giordano, F. Barone, F. Mazzei, and G. Chirico. 2004. Fluorescence anisotropy in the frequency domain by an optical microscope. *Appl. Spectrosc.* 58:160–165.

47. Lakowicz, J. R. 1999. Principles of Fluorescence Spectroscopy. Kluwer Academic/Plenum Publishers, Boston.

48. Dittrich, P. S., and P. Schwille. 2001. Photobleaching and stabilization of fluorophores used for single-molecule analysis with one- and two-photon excitation. *Appl. Phys. B.* 73:829–837.

49. Xie, X. S., and J. K. Trautman. 1998. Optical studies of single molecules at room temperature. *Annu. Rev. Phys. Chem.* 49:441–480.

50. Patterson, G. H., and D. W. Piston. 2000. Photobleaching in two-photon excitation microscopy. *Biophys. J.* 78:2159–2162.

51. Reference deleted in proof.

52. Abbruzzetti, S., E. Grandi, C. Viappiani, S. Bologna, B. Campanini, S. Raboni, S. Bettati, and A. Mozzarelli. 2005. Kinetics of acid-induced spectral changes in the GFPmut2 chromophore. *J. Am. Chem. Soc.* 127:626–635.

53. Bopp, N. A., Y. Jia, G. Haran, A. Morlino, and R. M. Hochstrasser. 1998. Single-molecule spectroscopy with 27 fs pulses: time-resolved experiments and direct imaging of orientational distributions. *Appl. Phys. Lett.* 73:7–9.

54. Zimmer, M. 2002. Green fluorescent protein (GFP): applications, structure, and related photophysical behavior. *Chem. Rev.* 102:759–781.

55. Teeter, M. M., A. Yamano, B. Stec, and U. Mohanty. 2001. On the nature of a glassy state of matter in a hydrated protein: relation to protein function. *Proc. Natl. Acad. Sci. USA.* 98:11242–11247.

56. Ediger, M. D. 2000. Spatially heterogeneous dynamics in supercooled liquids. *Annu. Rev. Phys. Chem.* 51:99–128.

57. Roberts, C. J., and P. G. Debenedetti. 1999. Structure and dynamics in concentrated, amorphous carbohydrate-water systems by molecular dynamics simulation. *J. Phys. Chem. B.* 103:7308–7318.

58. Talaga, D. S., W. L. Lau, H. Roder, J. Tang, Y. Jia, W. F. DeGrado, and R. M. Hochstrasser. 2000. Dynamics and folding of single two-stranded coiled-coil peptides studied by fluorescent energy transfer confocal microscopy. *Proc. Natl. Acad. Sci. USA.* 97:13021–13026.